Dissipative Effects in the Electronic Transport through DNA Molecular Wires

R. Gutiérrez,* S. Mandal, and G. Cuniberti
Institute for Theoretical Physics, University of Regensburg, D-93040 Regensburg, Germany
(Dated: March,04 2005)

We investigate the influence of a dissipative environment which effectively comprises the effects of counterions and hydration shells, on the transport properties of short DNA wires. Their electronic structure is captured by a tight-binding model which is embedded in a bath consisting of a collection of harmonic oscillators. Without coupling to the bath a temperature independent gap opens in the electronic spectrum. Upon allowing for electron-bath interaction the gap becomes temperature dependent. It increases with temperature in the weak-coupling limit to the bath degrees of freedom. In the strong-coupling regime a bath-induced *pseudo-gap* is formed. As a result, a crossover from tunneling to activated behavior in the low-voltage region of the I-V characteristics is observed with increasing temperature. The temperature dependence of the transmission near the Fermi energy, $t(E_{\rm F})$, manifests an Arrhenius-like behavior in agreement with recent transport experiments. Moreover, $t(E_{\rm F})$ shows a weak exponential dependence on the wire length, typical of strong incoherent transport. Disorder effects smear the electronic bands, but do not appreciably affect the pseudo-gap formation.

PACS numbers: 87.14.Gg,87.15.-v 73.63.-b,71.38.-k 72.20.Ee,72.80.Le, 05.60.Gg

I. INTRODUCTION

The idea that conduction pathways in DNA molecules may be built up as a result of the hybridization of the π orbital stack along consecutive base pairs can be traced back to the 1960's.[1] It was not, however, till recently that a revival of interest on DNA as a potential conductor occurred. This was mainly triggered by the observation of long-range electron transfer between intercalated donor and acceptor centers in DNA molecules in solution.[2] Subsequent experimental results[3,4,5,6,7,8,9] were controversial as they showed different functional dependences of electron transfer rates on the donor-acceptor separation. Thus, strong exponential fall-off[4,5] typical for superexchange mediated transfer as well as a weak, algebraic dependence[3,8] characteristic of sequential hopping processes were reported. Meanwhile, theoretical work has led to an emerging picture where different mechanisms may coexist depending on base-pair sequence and energetics.[10,11]

In parallel to these developments in the chemical physics community, DC transport experiments on λ-DNA as well as on poly(dG)-poly(dC) and poly(dA)-poly(dT) molecules between metal electrodes have been performed.[12,13,14,15,16,17,18,19] Several fundamental difficulties have to be surmounted in this kind of experiments: (i) how to create good contacts to the metal electrodes, (ii) how to control charge injection into the molecule, (iii) single molecule vs. bundles of molecules and (iv) dry vs. aqueous environments, among others. Consequently, sample preparation and the specific experimental conditions turn out to be very critical for DNA transport measurements. Thus, experiments have yielded contradictory results as to the conduction properties of DNA and are rather difficult to analyze. DNA has been characterized as a pure insulator,[14,16] as a wide-band gap semiconductor,[13] and as a metallic system.[12,20] Especially interesting are recent transport measurements on single poly(dG)-poly(dC) oligomers in aqueous solution, which displayed metallic-like I-V characteristics and an algebraic behavior in the length dependence of the conductance.[20]

Notwithstanding this variety of results and the problems related to the experimental set-up, the possibility of using DNA in molecular electronics is extremely attractive since it would open a vast range of potential applications because of its self-assembling and recognition properties.[14] Alternatively, DNA can also be used as a template in molecular electronic devices.[21,22,23]

From a theoretical point of view, the knowledge of the electronic structure of the base-pairs, the sugar/phosphate mantle and their mutual interactions is required in order to clarify the transport processes that may be effective in DNA. First principle approaches are the most suitable tools for this goal. However, the huge complexity of this molecule makes *ab initio* calculations still very demanding, so that only few investigations have been performed, mainly in well-stacked periodic structures.[24,25,26,27,28,29,30,31,32,33,34] To complicate this picture, environmental effects such as the presence of water molecules and counterions which stabilize the molecular structure make *ab initio* calculations even more challenging.[26,27] Hence, Hamiltonian models[36,37,38,39,40,41,42,43,44,45] that isolate single factors affecting electron transport are still playing a significant role and can help to shed more light onto the above issues as well as guide first principle investigations.

Recently, Cuniberti *et al.*[41] proposed a minimal model Hamiltonian to explain the semiconducting behavior previously observed by Porath *et al.*[13] in suspended short (up to 30 base-pairs) poly(dG)-poly(dC) molecules. Remarkably enough, this experiment was performed on single molecules, in contrast to most transport experiments involving bundles of molecules. Molecular systems like Poly(dG)-poly(dC) (or Poly(dA)-poly(dT)) are very at-

tractive from a theoretical standpoint since, being periodic, band-like transport as a result of π-orbitals hybridization may be more efficient than in its strongly disordered counterparts, *e.g.* in λ-DNA. The above model[41] mimics the electronic structure of the complex poly(dG)-poly(dC)-backbone system by a tight-binding chain to which side chains are attached. Electrons can hop along the central chain but not along the side chains. As a result a gap in the electronic spectrum opens. The gap is obviously temperature independent and the transmission near the Fermi level would show a strong exponential dependence due to the absence of electronic states to support transport.

An immediate issue that arises is how stable this electronic structure, *i.e.* two electronic bands separated by a gap, is against the influence of several factors which are known to play an important role in controlling charge propagation in DNA molecules, such as static and dynamic disorder[47,48,49,50,51,52,53] and environment.[26,27,40] In particular, the environment can act as a source of decoherence for a propagating electron (or hole),[40] it can induce structural fluctuations that support or restrict charge motion,[26] or it can introduce additional electronic states within the fundamental gap.[19,27] As it has been demonstrated experimentally, a modification of the humidity causes variations of orders of magnitude in the conductivity of DNA.[54,55] Moreover, the recent single-molecule experiments of Xu *et al.*[20] suggest that the environment may strongly modified the low-bias transport properties of DNA oligomers.

In this paper we elaborate on the role played by the environment by addressing signatures of the bath in the electronic transmission spectrum of the DNA wire in different coupling regimes: the mean-field approximation as well as weak-coupling and strong-coupling limits. Anticipating some of our results, we find that the semiconducting gap *closes* on the mean-field level as a result of thermal fluctuations. In the weak-coupling limit, however, the gap *opens* with increasing temperature. In both cases the electronic gap is an "intrinsic" property of the system. On the contrary, a bath-induced *pseudo-gap* is formed in the strong coupling limit, *i.e.* an energy region with a low (but finite) density of electronic states. We have further found in this regime that the transmission at the Fermi level exponentially decreases with the wire length L, $t(E_{\rm F}) \sim {\rm e}^{-\gamma L}$. The decay rate γ is however rather small ~ 0.2 Å^{-1}. This together with a noticeable dependence of γ on the electron-bath coupling clearly indicates that incoherent pathways do appreciably contribute to charge transport in the strong coupling limit.

In the next section we introduce the model Hamiltonian and derive the corresponding Green functions which are required to calculate the linear conductance. In section III different approximation schemes associated with different coupling regimes to the bath are discussed. The influence of structural disorder on our results is also presented. Finally, our summary follows in section IV.

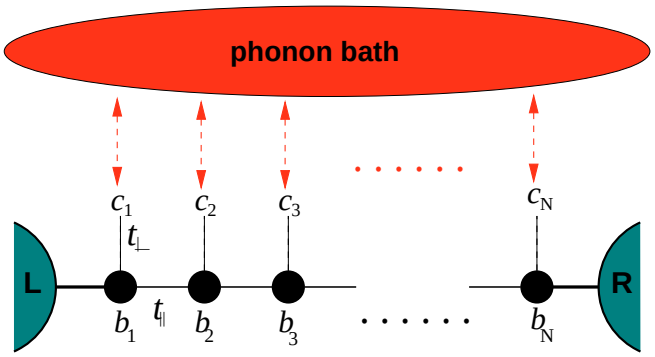

FIG. 1: (Color line) Schematic drawing of the DNA molecular wire in contact with a dissipative environment. The central chain with N sites is connected to semiinfinite left (L) and right (R) electronic reservoirs. The bath only interacts with the side chain sites (c), which we call backbone sites.[56] The Hamiltonian associated with this model is given by Eqs. (1), (2), and (3) in the main text.

II. HAMILTONIAN MODEL

Along the lines of Refs. 41, we represent the DNA molecular wire containing N base pairs by the following nearest-neighbour tight-binding Hamiltonian (see Fig. 1):

$$\begin{aligned}\mathcal{H}_{\rm el} &= \epsilon_b \sum_j b_j^\dagger b_j - t_{||} \sum_j \left[b_j^\dagger b_{j+1} + {\rm H.c.} \right] \\ &+ \epsilon \sum_j c_j^\dagger c_j \\ &- t_\perp \sum_j \left[b_j^\dagger c_j + {\rm H.c.} \right] \\ &= \mathcal{H}_{\rm C} + \mathcal{H}_{\rm b} + \mathcal{H}_{\rm C\text{-}c}. \end{aligned} \tag{1}$$

Hereby $\mathcal{H}_{\rm C}$ and $\mathcal{H}_{\rm b}$ are the Hamiltonians of the central and side chains, respectively, and $\mathcal{H}_{\rm C\text{-}b}$ is the coupling between them. $t_{||}$ and $t_\perp$ are hopping integrals along the central chain and between the backbone sites and the central chain, respectively. If not stated otherwise, the on-site energies will be later set equal to zero. The $\mathcal{H}_{\rm C}$ Hamiltonian can be considered as effectively modeling one of the frontier orbitals of the poly(dG)-poly(dC) system, *e.g.* the highest-occupied molecular orbital, which is localized on the guanine bases.[27,28] The side chain induces then a perturbation of the π-stack leading to the opening of a temperature independent semiconducting gap in the electronic spectrum, the gap being proportional to the transversal hopping integral $t_\perp$.[41] Since this model shows electron-hole symmetry, two electronic manifolds containing N states each, are symmetrically situated around the Fermi level, which is taken as the zero of energy.

We focus here on the influence of the environment on the electronic structure and consequently on the transport properties of the model described by $\mathcal{H}_{\rm el}$. As it has been demonstrated in the past years, correlated fluctuations

of hydrated counterions strongly influence electron(hole) motion along the double-helix.[19,26] Recent Raman and neutron scattering experiments on lysozyme have shown that the protein dynamics follows the solvent dynamics over a broad temperature range. Especially, conformational changes, low-energy vibrational excitations and the corresponding temperature dependences turned out to be very sensitive to the solvents dynamics.[57] We consider the vibrational degrees of freedom of counterions and hydration shells in DNA as a dynamical bath able to act as a dissipative environment. In this model Hamiltonian approach, we do not consider specific features of the environment but represent it by a phonon bath of M harmonic oscillators. We further make the assumption that the bath is only directly affecting the side chain whereas the central chain is well screened by the latter. Then, the extended Hamiltonian becomes:

$$\begin{aligned}\mathcal{H}_{\rm W} &= \mathcal{H}_{\rm el} + \sum_{\alpha} \Omega_\alpha B_\alpha^\dagger B_\alpha + \sum_{\alpha,j} \lambda_\alpha c_j^\dagger c_j (B_\alpha + B_\alpha^\dagger) \\ &= \mathcal{H}_{\rm el} + \mathcal{H}_{\rm B} + \mathcal{H}_{\rm c\text{-}B}, \end{aligned} \tag{2}$$

where $\mathcal{H}_{\rm B}$ and $\mathcal{H}_{\rm c\text{-}B}$ are the phonon bath Hamiltonian and the backbone-bath interaction, respectively. B_α is a bath phonon operator and λ_α denotes the electron-phonon coupling. Note that we assume a local coupling of the bath modes to the electronic density at the side chain. Later on, the thermodynamic limit ($M \to \infty$) in the bath degrees of freedom will be carried out and the corresponding bath spectral density introduced, so that at this stage we do not need to further specify the set of bath frequencies Ω_α and coupling constants λ_α.

Finally, we include the coupling of the molecular wire to semiinfinite left (L) and right (R) electrodes:

$$\begin{aligned}\mathcal{H} &= \mathcal{H}_{\rm W} + \sum_{\mathbf{k}\in{\rm L,R},\sigma} \epsilon_{\mathbf{k}\sigma} d_{\mathbf{k}\sigma}^\dagger d_{\mathbf{k}\sigma} \\ &\quad + \sum_{\mathbf{k}\in{\rm L},\sigma} (V_{\mathbf{k},1}\, d_{\mathbf{k}\sigma}^\dagger\, b_1 + {\rm H.c.}) \\ &\quad + \sum_{\mathbf{k}\in R,\sigma} (V_{\mathbf{k},N}\, d_{\mathbf{k}\sigma}^\dagger\, b_N + {\rm H.c.}) \\ &= \mathcal{H}_{\rm W} + \mathcal{H}_{\rm L/R} + \mathcal{H}_{\rm L\text{-}C} + \mathcal{H}_{\rm R\text{-}C} \end{aligned} \tag{3}$$

The Hamiltonian of Eq. (3) is the starting point of our investigation. Performing the Lang-Firsov[59] unitary transformation $\bar{\mathcal{H}} = {\rm e}^{\,S}\mathcal{H}{\rm e}^{\,-S}$ with the generator $S = \sum_{\alpha,j}(\lambda_\alpha/\Omega_\alpha)c_j^\dagger c_j(B_\alpha - B_\alpha^\dagger)$ and $S^\dagger = -S$, the linear coupling to the bath can be eliminated. In the resulting effective Hamiltonian only the backbone part is modified since the central chain operators b_ℓ as well as the leads' operators $d_{\mathbf{k}\sigma}$ are invariant with respect to the above transformation. The new Hamiltonian reads:

$$\begin{aligned}\bar{\mathcal{H}} &= \mathcal{H}_{\rm C} + \mathcal{H}_{\rm L/R} + \mathcal{H}_{\rm B} + \mathcal{H}_{\rm L/R\text{-}C} \\ &\quad + (\epsilon - \Delta)\sum_j c_j^\dagger c_j - t_\perp \sum_j \Big[b_j^\dagger c_j \mathcal{X} + {\rm H.c.}\Big] \qquad (4) \\ \mathcal{X} &= \exp\left[\sum_\alpha \frac{\lambda_\alpha}{\Omega_\alpha}(B_\alpha - B_\alpha^\dagger)\right], \quad \Delta = \sum_\alpha \frac{\lambda_\alpha^2}{\Omega_\alpha}. \end{aligned}$$

Let's define two kinds of retarded thermal Green functions related to the central chain $G_{j\ell}(t)$ and to the backbones $P_{j\ell}(t)$, respectively ($\hbar = 1$):

$$\begin{aligned} G_{j\ell}(t) &= -i\Theta(t)\left\langle \Big[b_j(t), b_\ell^\dagger(0)\Big]_+ \right\rangle, \qquad (5) \\ P_{j\ell}(t) &= -i\Theta(t)\left\langle \Big[c_j(t)\mathcal{X}(t), c_\ell^\dagger(0)\mathcal{X}^\dagger(0)\Big]_+ \right\rangle, \end{aligned}$$

where Θ is the Heaviside function and the average is taken w.r.t. $\bar{\mathcal{H}}$. With the above definitions and using the equation of motion technique (see Appendix A) we arrive to an expression for the Fourier transform of the central chain Green function which reads, to lowest-order in $t_\perp$:

$$\begin{aligned} \mathbf{G}^{-1}(E) &= \mathbf{G}_0^{-1}(E) - t_\perp^2 \mathbf{P}(E) \qquad (6) \\ \mathbf{G}_0^{-1}(E) &= E\mathbf{1} - \mathcal{H}_{\rm C} - \Sigma_{\rm L}(E) - \Sigma_{\rm R}(E). \end{aligned}$$

In this equation $\mathbf{G}_0(E)$ is the Green function of a chain without backbones and connected to the left and right electrodes. The influence of the latter is comprised in the complex self-energy functions $\Sigma_{\rm L/R}(E)$.[60] The polaronic Green function $\mathbf{P}(E)$ is explicitly given by:

$$\begin{aligned} P_{\ell j}(E) &= -{\rm i}\,\delta_{\ell j}\int_0^\infty {\rm d}t\, {\rm e}^{\,{\rm i}\,(E+{\rm i}\,0^+)t}\, {\rm e}^{\,-{\rm i}\,(\epsilon-\Delta)\,t} \\ &\quad \times \Big[(1-f_{\rm c}){\rm e}^{\,-\Phi(t)} + f_{\rm c}{\rm e}^{\,-\Phi(-t)}\Big] \end{aligned} \tag{7}$$

with ${\rm e}^{\,-\Phi(t)} = \big\langle \mathcal{X}(t)\mathcal{X}^\dagger(0)\big\rangle_{\rm B}$ being a dynamical bath correlation function. The average $\langle\cdot\rangle_{\rm B}$ is performed over the bath degrees of freedom. Working to lowest order in $t_\perp$ allows to use a zero-order Green function for the side chain in Eq. (7), *i.e.* $G_{0,\ell j}^{\rm c}(t) \sim \delta_{\ell j}{\rm e}^{\,-{\rm i}\,(\epsilon-\Delta)\,t}$. $f_{\rm c}$ is the Fermi function at the backbone sites. In what follows we consider the case of empty sites by setting $f_{\rm c} = 0$. Note that $\mathbf{P}$ is a diagonal matrix, *i.e.* it only modifies the on-site energies in the Hamiltonian.

In order to get closed expressions for the bath thermal averages it is appropriate to introduce a bath spectral density[58] defined by :

$$J(\omega) = \sum_\alpha \lambda_\alpha^2 \delta(\omega - \Omega_\alpha) = J_0(\frac{\omega}{\omega_{\rm c}})^s {\rm e}^{\,-\omega/\omega_{\rm c}}\Theta(\omega), \tag{8}$$

where $\omega_{\rm c}$ is a cut-off frequency related to the bath memory time $\tau_{\rm c} \sim \omega_{\rm c}^{-1}$. It is easy to show that the limit $\omega_{\rm c} \to$

∞ corresponds to a Markovian bath, *i.e.* $J(t) \sim J_0\delta(t)$. Using this *Ansatz*, $\Phi(t)$ can be written in the usual way:[58]

$$\Phi(t) \;=\; \int_0^\infty \mathrm{d}\omega\, \frac{J(\omega)}{\omega^2}\left[1-\mathrm{e}^{-\mathrm{i}\,\omega t}+2\frac{1-\cos\omega t}{\mathrm{e}^{\,\beta\omega}-1}\right]. \quad (9)$$

Although the integral can be performed analytically[58], we consider $\Phi(t)$ in some limiting cases where it is easier to work directly with Eq. (9).

In the transport calculations, we limit ourselves to treat the low voltage regime, thus neglecting non-equilibrium effects as well as the inelastic part of the total current. As a result, one can still define a linear conductance g as follows:[61]

$$g(E) \;=\; \frac{2e^2}{h}\int dE\left(-\frac{\partial f}{\partial E}\right) t(E), \quad (10)$$
$$t(E) \;=\; \mathrm{Tr}\left\{\mathbf{\Delta}_{\mathrm{L}}\,\mathbf{G}\,\mathbf{\Delta}_{\mathrm{R}}\,\mathbf{G}^{\dagger}\right\},$$

where $\mathbf{\Delta}_{\mathrm{L,R}} = \mathrm{i}\left(\mathbf{\Sigma}_{\mathrm{L,R}} - \mathbf{\Sigma}^{\dagger}_{\mathrm{L,R}}\right)$ are spectral densities of the leads. Although the foregoing expression is similar to Landauer's formula, we stress that the influence of the phonon bath does implicitly appear via the Green function $\mathbf{G}$. Hence, both coherent *and* incoherent pathways for charge transport mediated by phonon processes are included in Eq. (10). We concentrate our discussion on the temperature and length dependence of $t(E)$. In what follows we always plot $t(E)$ rather than g to filter out temperature effects arising from the derivative of the Fermi function in Eq. (10). For completeness the current as given by $I(V) = (2e/h)\int \mathrm{d}E\,(f(E-eV/2) - f(E+eV/2))t(E)$ is also shown. We remark however, that this expression neglects non-equilibrium effects, which are beyond the scope of this investigation.

III. LIMITING CASES

We use now the results of the foregoing section to discuss the electronic transport properties of our model in some limiting cases for which analytic expressions can be derived. In all cases, we use the wide-band limit in the electrode selfenergies, *i.e.* $\Sigma_{\mathrm{L},\ell j}(E) = -\mathrm{i}\,\Gamma_{\mathrm{L}}\delta_{1\ell}\delta_{1j}$ and $\Sigma_{\mathrm{R},\ell j}(E) = -\mathrm{i}\,\Gamma_{\mathrm{R}}\delta_{N\ell}\delta_{Nj}$. We discuss the mean-field approximation and the weak-coupling regime in the electron-bath interaction as well as the strong-coupling limit. Farther, the cases of ohmic ($s=1$) and superohmic ($s=3$) spectral densities are treated.

A. Mean-field approximation (MFA)

Within the mean-field approximation bath fluctuations contained in $P(E)$ are neglected. The MFA can be introduced by writing the phonon operator $\mathcal{X}$ as $\langle\mathcal{X}\rangle_{\mathrm{B}} + \delta\mathcal{X}$ in $\mathcal{H}_{\text{C-c}}$ in Eq. (4), *i.e.* $\mathcal{H}^{\mathrm{MF}}_{\text{C-c}} = -t_\perp\sum_j\left[b_j^\dagger c_j\,\langle\mathcal{X}\rangle_{\mathrm{B}} + \mathrm{H.c.}\right] +$

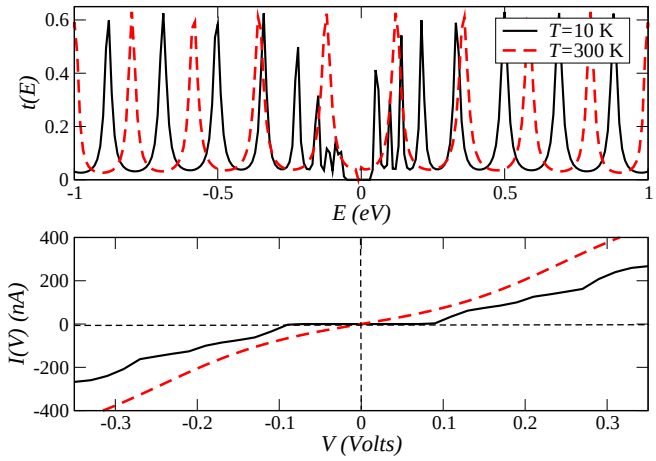

FIG. 2: (Color online) Electronic transmission and corresponding current in the mean-field approximation for two different temperatures. Parameters: $N = 20, J_0/\omega_{\mathrm{c}} = 0.12, t_\perp/t_{||} = 0.5, \Gamma_{\mathrm{L/R}}/t_{||} = 0.5$.

$O(\delta\mathcal{X})$. As a result a real, static and temperature dependent term in Eq. (6) is found:

$$\mathbf{G}^{-1}(E) = \mathbf{G}_0^{-1}(E) - t_\perp^2\frac{|\,\langle\mathcal{X}\rangle_{\mathrm{B}}\,|^2}{E-\epsilon+\Delta+\mathrm{i}\,0^+}\mathbf{1}, \quad (11)$$

where $|\langle\mathcal{X}\rangle_{\mathrm{B}}|^2 = \mathrm{e}^{\,-2\kappa(T)}$ and $\kappa(T)$ is given by:

$$\kappa(T) = \int_0^\infty \frac{\mathrm{d}\omega}{\omega^2}J(\omega)\coth\frac{\omega}{2k_{\mathrm{B}}T}. \quad (12)$$

The effect of the MF term is thus to scale the bare transversal hopping $t_\perp$ by the exponential temperature dependent factor $\mathrm{e}^{\,-\kappa(T)}$.

In the case of an ohmic bath, $s=1$, the integrand in $\kappa(T)$ scales as $1/\omega^p$, $p=1,2$ and has thus a logarithmic divergence at the lower integration limit, see Eqs. (8) and (12). Thus, the MF contribution would vanish. In other words, no gap would exist on this approximation level.

In the superohmic case ($s=3$) all integrals are regular. One obtains $\Delta = \int \mathrm{d}\omega\,\omega^{-1}J(\omega) = \Gamma(s-1)J_0 = 2J_0$, with $\Gamma(s)$ being the Gamma function and $\kappa(T)$ reads:

$$\kappa(T) = \frac{2J_0}{\omega_{\mathrm{c}}}\left[2\left(\frac{k_{\mathrm{B}}T}{\omega_{\mathrm{c}}}\right)^2\zeta_{\mathrm{H}}\left(2,\frac{k_{\mathrm{B}}T}{\omega_{\mathrm{c}}}\right)-1\right]. \quad (13)$$

$\zeta_{\mathrm{H}}(s,z) = \sum_{n=0}^\infty (n+z)^{-s}$ is the Hurwitz ζ-function, a generalization of the Riemann ζ-function.[62]

It follows from Eq. (13) that $\kappa(T)$ behaves like a constant for low temperatures ($k_{\mathrm{B}}T/\omega_{\mathrm{c}} < 1$), $\kappa(T) \sim J_0/\omega_{\mathrm{c}}$, while it scales linear with T in the high-temperature limit ($k_{\mathrm{B}}T/\omega_{\mathrm{c}} > 1$), $\kappa(T) \sim J_0/\omega_{\mathrm{c}}(1 + 2k_{\mathrm{B}}T/\omega_{\mathrm{c}})$.

If J_0 vanishes, Δ is zero and $\langle\mathcal{X}\rangle_{\mathrm{B}} = 1$. Thus we recover the original model of Ref. 41 which has a gap proportional to $t_\perp$. For $J_0 \neq 0$ and at zero temperature the hopping integral is roughly reduced to $t_\perp\mathrm{e}^{\,-\frac{J_0}{\omega_{\mathrm{c}}}}$ which

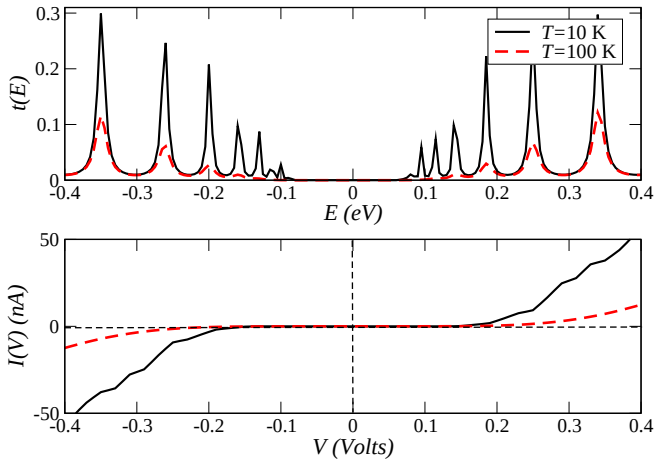

FIG. 3: (Color line) Electronic transmission and corresponding current in the weak-coupling limit with ohmic dissipation ($s = 1$) in the bath. Parameters: $N = 20, J_0/\omega_c = 0.2, t_\perp/t_{||} = 0.6, \Gamma_{L/R}/t_{||} = 0.5$

is similar to the renormalization of the hopping in Holstein's polaron model,[63] though here it is $t_\perp$ rather than $t_{||}$ the term that is rescaled. At high temperatures $t_\perp$ is further reduced ($\kappa(T) \sim T$) so that the gap in the electronic spectrum finally collapses and the system becomes metallic, see Fig. 2. An appreciable temperature dependence can only be observed in the limit $J_0/\omega_c < 1$; otherwise the gap would collapse already at zero temperature due to the exponential dependence on J_0. We further remark that the MFA may be only valid in the regime $J_0/\omega_c < 1$, $k_B T/\omega_c \lesssim 1$, otherwise multiphonon processes in the bath, which are not considered at this stage, become increasingly relevant.

B. Beyond MF: weak-coupling limit

As a first step beyond the mean-field approach let's first consider the weak-coupling limit in $\mathbf{P}(E)$. For $J_0/\omega_c < 1$ and not too high temperatures ($k_B T/\omega_c \lesssim 1$) the main contribution to the integral in Eq. (7) comes from long times $t \gg \omega_c^{-1}$. With the change of variables $z = \omega t$, $\Phi(t)$ can be written as:

$$\Phi(t) = J_0 \omega_c^{-s} t^{1-s} \int_0^\infty \mathrm{d}z\, z^{s-2} \mathrm{e}^{-\frac{z}{\omega_c t}} \times \left(1 - \mathrm{e}^{-\mathrm{i}\, z} + 2\frac{1-\cos z}{\mathrm{e}^{z\frac{\beta\omega_c}{\omega_c t}} - 1}\right). \quad (14)$$

As far as $\omega_c t \gg \beta\omega_c$ this can be simplified to:

$$\Phi(t) \approx J_0 \omega_c^{-s} t^{1-s} \int_0^\infty \mathrm{d}x\, z^{s-2} \mathrm{e}^{-\frac{z}{\omega_c t}} \times \left(1 - \mathrm{e}^{-\mathrm{i}\, z} + 2\frac{\beta\omega_c}{\omega_c t}\frac{1-\cos z}{z}\right). \quad (15)$$

Since in the long-time limit the low-frequency bath modes are giving the most important contribution we may expect some qualitative differences in the ohmic and superohmic regimes. For $s = 1$ we obtain $\Phi(t) \sim \pi \frac{J_0}{\omega_c} \frac{k_B T}{\omega_c} (\omega_c t)$ which leads to (using $\Delta(s = 1) = J_0$):

$$\mathbf{G}^{-1}(E) = \mathbf{G}_0^{-1}(E) - t_\perp^2 \frac{1}{E + J_0 + \mathrm{i}\,\pi \frac{J_0}{\omega_c} k_B T} \mathbf{1}, \quad (16)$$

i.e. there is only a pure imaginary contribution from the bath. For the simple case of a single site coupled to a backbone one can easily see that the gap approximately scales as $\sqrt{k_B T}$; thus it grows with increasing temperature. This is shown in Fig. 3, where we also see that the intensity of the transmission resonances strongly goes down with increasing temperature. The gap enhancement is induced by the suppression of the transmission peaks of the frontier orbitals, i. e. those closest to the Fermi energy.

For $s = 3$ and $k_B T/\omega_c \lesssim 1$, $\Phi(t)$ takes a nearly temperature independent value proportional to J_0/ω_c. As a result the gap is slightly reduced ($t_\perp \to t_\perp \mathrm{e}^{-J_0/\omega_c}$) but, because of the weak-coupling condition, the effect is rather small.

From this discussion we can conclude that in the weak-coupling limit ohmic dissipation in the bath induces an enhancement of the electronic gap while superohmic dissipation does not appreciably affect it. In the high-temperature limit $k_B T/\omega_c > 1$ a short-time expansion can be performed which yields similar results to those of the strong-coupling limit (see next section),[42] so that we do not need to discuss them here. Note farther that the gap obtained in the weak-coupling and mean-field limits is an "intrinsic" property of the electronic system; it is only quantitatively modified by the interaction with the bath degrees of freedom. We thus trivially expect a strong exponential dependence of $t(E = E_F)$ on the wire length, typical of virtual tunneling through a gap. Indeed, we find $t(E = E_F) \sim \exp(-\beta L)$ with $\beta \sim 2 - 3\,\mathring{A}^{-1}$.

C. Beyond MF: strong coupling limit (SCL)

In this section we discuss the strong-coupling regime, as defined by the condition $J_0/\omega_c > 1$. This may be the regime to be found in presence of an aqueous environment, as recent theoretical estimations using the classical Onsager model for solvation processes have shown.[64] In the SCL the main contribution to the time integral in Eq. (7) arises from short times. Hence a short-time expansion of $\Phi(t)$ may already give reasonable results and it allows, additionally, to find an analytical expression for

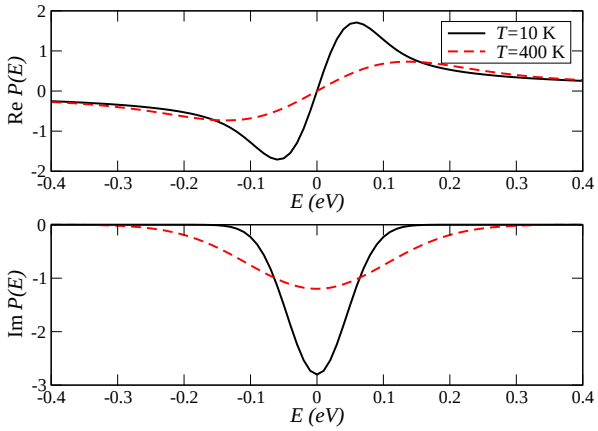

FIG. 4: (Color line) Temperature dependence of the real and imaginary parts of $P(E)$ for $N = 20$, $J_0/\omega_c = 10, t_\perp/t_{||} = 0.4, \Gamma_{L/R}/t_{||} = 0.5$. With increasing temperature the slope of the real part near $E = 0$ decreases and the imaginary part broadens and loses intensity. A similar qualitative dependence on J_0 was found (not shown).

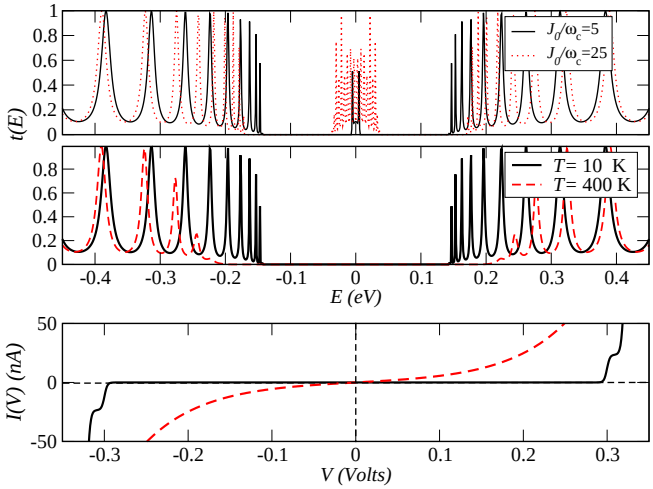

FIG. 5: (Color line) Upper panel: $t(E)$ with $\mathrm{Im}\, P(E) = 0$; the intensity of the resonances on the central narrow band is strongly dependent on J_0/ω_c and $k_B T$ (not shown). Temperature dependence of $t(E)$ with full inclusion of $P(E)$ (middle panel) and corresponding current (lower panel) for $N = 20$, $J_0/\omega_c = 5, t_\perp/t_{||} = 0.5, \Gamma_{L/R}/t_{||} = 0.2$. The pseudo-gap increases with temperature.

$\mathbf{P}(E)$. At $t \ll \omega_c^{-1}$ we find,

$$\begin{aligned}
\Phi(t) &\approx \mathrm{i}\,\Delta\, t + (\omega_c t)^2\, \kappa_0(T) \qquad (17)\\
P_{\ell j}(E) &= -\mathrm{i}\,\delta_{\ell j} \int_0^\infty \mathrm{d}t\, \mathrm{e}^{\,\mathrm{i}\,(E-\epsilon+\mathrm{i}\,0^+)t}\, \mathrm{e}^{\,-(\omega_c t)^2 \kappa_0(T)}\\
&= -\mathrm{i}\,\delta_{\ell j}\, \frac{\sqrt{\pi}}{2} \frac{1}{\omega_c \sqrt{\kappa_0(T)}}\, \exp\left(-\frac{(E-\epsilon+\mathrm{i}\,0^+)^2}{4\omega_c^2 \kappa_0(T)}\right)\\
&\quad \times \left(1 + \mathrm{erf}\left[\frac{\mathrm{i}\,(E-\epsilon+\mathrm{i}\,0^+)}{2\omega_c\sqrt{\kappa_0(T)}}\right]\right),\\
\kappa_0(T) &= \frac{1}{2\omega_c^2} \int_0^\infty \mathrm{d}\omega J(\omega) \coth \frac{\omega}{2k_B T}.
\end{aligned}$$

Before presenting the results for the electronic transmission, it is useful to first consider the dependence of the real and imaginary parts of $\mathbf{P}(E)$ on temperature and on the reduced coupling constant J_0/ω_c. Both functions are shown in Fig. 4. We see that around the Fermi level at $E = 0$ the real part is approximately linear, $\mathrm{Re}\, P(E) \sim E$ while the imaginary part shows a Gaussian-like behavior. The imaginary part loses intensity and becomes broadened with increasing temperature or J_0, while the slope in the real part decreases when $k_B T$ or J_0 are increased. If we neglect for the moment the imaginary part (the dissipative influence of the bath), we can understand the consequences of the real part being nonzero around the Fermi energy, *i.e.* in the gap region. The solutions of the non-linear equation $\det|(E - t_\perp^2\, \mathrm{Re}\, P(E))\mathbf{1} - \mathcal{H}_C| = 0$ give the new poles of the Green function of the system in presence of the phonon bath. For comparison, the equation determining the eigenstates *without* the bath is simply $\det|(E - t_\perp^2/E)\mathbf{1} - \mathcal{H}_C| = 0$. It is just the $1/E$ dependence near $E = 0$ that induces the appearance of two electronic bands of states separated by a gap.[41] In our present study, however, $\mathrm{Re}\, P(E \to 0)$ has no singular behavior and additional poles of the Green function may be expected to appear in the low-energy sector. This is indeed the case, as shown in Fig. 5 (upper panel). We find a third band of states around the Fermi energy, which we call a polaronic band because it results from the strong interaction between an electron and the bath modes. The intensity of this band as well as its band width strongly depend on temperature and on J_0. When $k_B T$ (or J_0) become large enough, these states spread out and eventually merge with the two other side bands. This would result in a transmission spectrum similar of a metallic system.

This picture is nevertheless not complete since the imaginary component of $P(E)$ has been neglected. Its inclusion leads to a dramatic modification of the spectrum, as shown in Fig. 5 (middle panel). We now only see two bands separated by a gap which basically resembles the semiconducting-type behavior of the original model. The origin of this gap or rather *pseudo-gap* (see below) is however quite different. It turns out that the imaginary part of $P(E)$, being peaked around $E = 0$, strongly suppresses the transmission resonances belonging to the central band. Additionally, the frontier orbitals on the side bands, *i.e.* orbitals closest to the gap region, are also strongly damped, this effect becoming stronger with increasing temperature ($\mathrm{Im}\, P(E)$ broadens). This latter effect has some similarities with the previously discussed weak-coupling regime. Note, however, that the new electronic manifold around the Fermi energy does not appear in the weak-coupling regime. We further stress that the density of states around the Fermi level is not exactly zero (hence the term pseudo-gap); the states on the polaronic manifold, although strongly damped, contribute nevertheless with a finite, temperature dependent

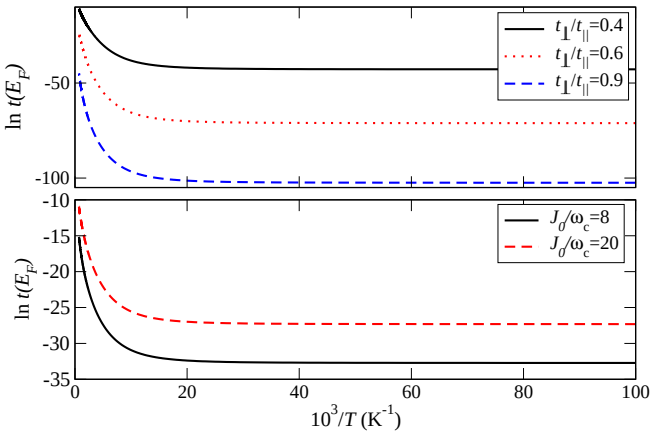

FIG. 6: (Color line) Arrhenius plot of $t(E = E_{\rm F})$ for different transversal couplings $t_\perp$ (upper panel) and electron-bath couplings $J_0/\omega_{\rm c}$ (lower panel). Parameters: $N = 20, t_\perp/t_{||} = 0.5, \Gamma_{\rm L/R}/t_{||} = 0.25$.

incoherent background to the transmission. As a result, with increasing temperature, a crossover from tunneling to activated behavior in the low-voltage region of the I-V characteristics takes place, see Fig. 5 (lower panel). The slope in the I-V plot becomes larger when $t_\perp$ is reduced, since the side bands approach each other and the effect of $\mathrm{Im}\, P(E)$ is reinforced.

In Fig. 6 an Arrhenius plot of the transmission at the Fermi energy is shown for different strengths of the transversal hopping integral and the electron-bath coupling. After a nearly T-independent region, the transmission strongly grows up following approximately a $\mathrm{e}^{-1/T}$ law. Increasing the coupling to the phonon bath makes the suppression of the polaronic band around $E = 0$ less effective ($\mathrm{Im}\, P(E \sim 0)$ decreases) so that the density of states around this energy becomes larger. Hence the absolute value of the transmission also increases. Similar T-dependences have been experimentally observed in poly(dG)-poly(dC)[12] as well as in λ-DNA.[17] On the other side, increasing $t_\perp$ leads to a reduction of the transmission at the Fermi level, since the energetic separation of the side bands increases with $t_\perp$.

We have further investigated the length dependence of the transmission at the Fermi energy. This is a very important aspect that helps to identify the influence of different transport mechanisms.[11,65] The results are displayed in Fig. 7 for different values of the reduced coupling $J_0/\omega_{\rm c}$. For a homogeneous chain (on-site energies are set to zero) an exponential dependence on the chain length $t(E_{\rm F}) \sim \mathrm{e}^{-\gamma L}$ was found. In this expression $L = Na_0$, where N is the number of sites on the molecular wire and $a_0 \sim 3.4\,$Å is the average distance between consecutive base pairs. Note that the inverse decay lengths γ are rather small $\sim 0.1 - 0.3\,\text{Å}^{-1}$. An exponential dependence usually indicates virtual tunneling through a gap. Inverse decay lengths, as extracted e. g. from complex band structure calculations,[34,35] are however much larger that those obtained in the present investigation. So have recent DFT-based calculations found values of $\gamma \sim 1.5\,\text{Å}^{-1}$ for gap tunneling in dry Poly(dG)-Poly(dC) oligomers.[34] With increasing bath coupling the exponential dependence farther weakens and eventually becomes algebraic $t(E_{\rm F}) \sim N^{-\alpha}$. The introduction of a tunnel barrier as realized *e.g.* through insertion of $(\mathrm{AT})_n$ groups, by shifting the on-site energies along a finite segment of the chain increases the inverse decay length γ by a factor of 2, approximately. Obviously, this model cannot describe the crossover from superexchange mediated electron transfer (strong exponential behavior) to sequential hopping-mediated transport (algebraic dependence) as a function of the *wire length* N, as discussed in other works.[11,65] We guess that vibrational excitations inside the central chain, which renormalize the longitudinal hopping integral $t_{||}$, have to be included to get this non-monotonic transition.

From the previous discussion we may conclude that electron transport on the low-energy sector of the transmission spectrum is supported by the formation of polaronic states. Though strongly damped, these states manifest nonetheless with a finite density of states inside the bandgap.

It has been meanwhile demonstrated[26,48,49,50,51,52,53] that electron (or hole) motion in DNA is extremely sensitive to different kinds of disorder: static disorder (random base-pair sequences), structural fluctuations and inhomogeneities of the counterions distribution along the backbones. These factors may strongly distort the base pair stacking along the double helix and eventually affect the electronic transport properties. They deserve a separate study. However, as a test for the stability of our results we have randomly varied the on-site energies along the central chain by extracting them from a Gaussian distribution with variance σ_0. In this way we are simulating

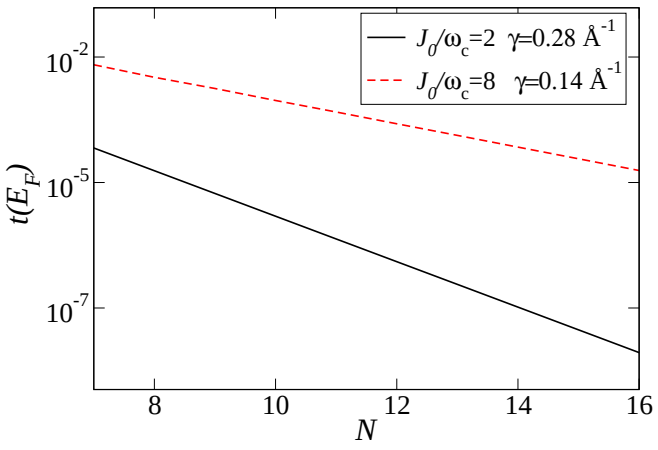

FIG. 7: (Color line) Chain length dependence of the transmission function at the Fermi energy for different electron-bath interaction strengths. Parameters: $t_\perp/t_{||} = 0.125, \Gamma_{\rm L/R}/t_{||} = 0.15, T = 200\,$K.

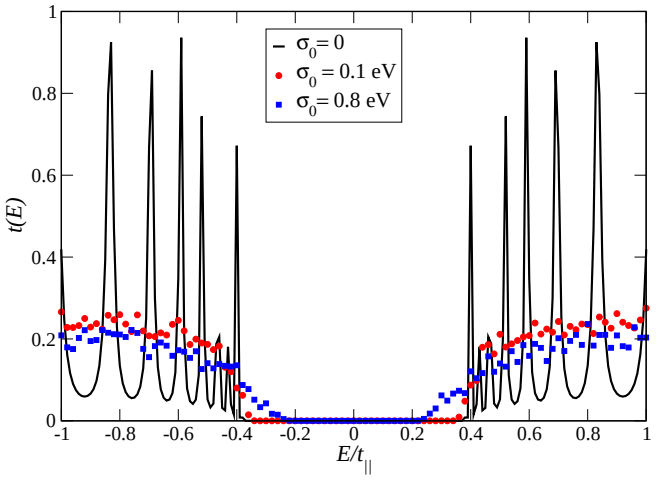

FIG. 8: (Color line) Transmission function in presence of thermal disorder in the central chain. Parameters: $N = 20, J_0/\omega_c = 5, t_\perp/t_{||} = 0.5, \Gamma_{L/R}/t_{||} = 0.15, T = 10$K. The transmission on the side bands decreases when the disorder becomes stronger, but the pseudo-gap is still seen, although it is partially reduced with increasing disorder.

fluctuations inside the central chain. In Fig. 8 the cases of weak ($\sigma_0 \sim 0.12 t_{||}$) and strong disorder ($\sigma_0 \sim t_{||}$) are shown. Two main features can be seen: (i) the transmission resonances on the side bands are strongly washed out and lose in intensity, and (ii) the pseudo-gap is slightly reduced with increasing disorder. However, the suppression of the central band due to $\mathrm{Im}\, P(E)$ and hence, the pseudo-gap formation is not affected by this kind of disorder. As soon as electronic states shift from the side bands into the region with nonzero $\mathrm{Im}\, P(E)$ they are strongly damped and thus the pseudo-gap structure of the spectrum is conserved. A similar effect of disorder is expected in the other coupling regimes to the bath degrees of freedom discussed above.

IV. SUMMARY

Charge propagation in DNA molecules is extremely sensitive to disorder and environmental effects. We have focused in this paper on the influence of a dissipative environment on the electronic transport properties of a model Hamiltonian which mimics some basic features of the electronic structure of DNA oligomers. Although we have chosen Poly(dG)-Poly(dC) molecules as a reference point, we believe that our model is quite generic and may be useful for a large class of π-conjugated systems.

We have shown that a mean-field approximation cannot fully catch the action of a dissipative environment on charge transport, because it only gives a real, energy independent contribution. Indeed, while the mean-field approach leads to gap reduction with increasing temperature, bath fluctuations eventually lead to gap opening in the weak-coupling limit. We have further shown that a bath-induced pseudo-gap in the electronic spectrum can appear for strong electron-bath coupling giving a temperature-dependent background around the Fermi energy. As a result the system may show with increasing temperature a transition from a tunneling to an activated behavior in the low-bias region when coupled to an external dissipative bath. An Arrhenius-like temperature dependence of the transmission at the Fermi level and a rather weak exponential dependence on the wire length were additionally found, indicating a strong contribution of incoherent pathways of the charge carriers.

A natural extension of this investigation would be the inclusion of non-equilibrium effects at large bias and consequently of inelastic components of the current. This issue is although interesting from a formal point of view, since the Lang-Firsov transformation introduces polaronic rather than pure electronic propagators, see Eq. (5). For the former the appropriate Keldysh Green functions should be derived in order to deal with the non-equilibrium regime. This problem deserves a separate investigation which is now in progress.

V. ACKNOWLEDGMENTS

We would like to thank M. Hartung and J. Keller for fruitful discussions. This work has been supported by the Volkswagen foundation and by the EU under contract IST-2001-38951.

APPENDIX A: DERIVATION OF EQ. (6)

The equation of motion for the retarded Green function in Eq. (5) in the frequency representation reads:

$$E G_{\ell j}(E) = \left\langle [b_j, b_\ell]_+ \right\rangle + ((\left[b_j, \bar{\mathcal{H}}\right] | b_\ell)).$$

Using it we get for the Hamiltonian of Eq. (3) :

$$\sum_n \left[G_0^{-1}(E)\right]_{\ell n} G_{nj}(E) = \delta_{\ell j} - t_\perp((c_\ell \mathcal{X} | b_j^\dagger)) \quad \text{(A1)}$$

$$\begin{aligned} \left[G_0^{-1}(E)\right]_{\ell n} &= (E - \epsilon_b)\delta_{n\ell} + t_{||}(\delta_{n,\ell+1} + \delta_{n,\ell-1}) \\ &\quad -\Sigma_L \delta_{\ell 1}\delta_{n1} - \Sigma_R \delta_{\ell N}\delta_{nN} \\ \Sigma_{L(R)} &= \sum_{\mathbf{k}\in L(R)} \frac{|V_{\mathbf{k},1(N)}|^2}{E - \epsilon_{\mathbf{k}} + \mathrm{i}0^+} \end{aligned}$$

Now, equations of motion from the "right" may be written for the Green function $Z^{\mathcal{X}}_{\ell j}(E) = ((c_\ell \mathcal{X} | b_j^\dagger))$, leading to :

$$\begin{aligned} \sum_m Z^{\mathcal{X}}_{\ell m}(E) \left[G_0^{-1}(E)\right]_{mj} &= -t_\perp((c_\ell \mathcal{X} | c_j^\dagger \mathcal{X}^\dagger)) \\ &= -t_\perp P_{\ell j}(E) \end{aligned} \quad \text{(A2)}$$

In the former equations we have neglected cross-terms of the form $((c_\ell \mathcal{X}|c_j^\dagger))$, since they will give contribution of $O(t_\perp^3)$. Inserting Eq. (A2) into Eq. (A1) we arrive at the matrix equation:

$$\mathbf{G}(E) = \mathbf{G}_0(E) + \mathbf{G}_0(E)\mathbf{\Sigma}_{\rm B}(E)\mathbf{G}_0(E),$$

which can be transformed into a Dyson-like equation when introducing the irreducible part $\mathbf{\Sigma}_{\rm B}(E) = \mathbf{\Sigma}_{\rm B}^{\rm irr}(E) + \mathbf{\Sigma}_{\rm B}^{\rm irr}(E)\mathbf{G}_0(E)\mathbf{\Sigma}_{\rm B}^{\rm irr}(E) + \ldots$:

$$\mathbf{G}(E) = \mathbf{G}_0(E) + \mathbf{G}_0(E)\mathbf{\Sigma}_{\rm B}^{\rm irr}(E)\mathbf{G}(E). \qquad \text{(A3)}$$

From Eq. (A3) it immediately follows Eq. (6) with $\mathbf{\Sigma}_{\rm B}^{\rm irr}(E) = t_\perp^2 \mathbf{P}(E)$. We emphasize that these expressions are exact only to lowest-order in the transversal hopping $t_\perp$. This approximation may be justified in the low-voltage limit we are dealing with.

* Electronic address: rafael.gutierrez@physik.uni-r.de

1 D. D. Eley and D. I. Spivey, Trans. Faraday Soc. **58**, 411 (1962).
2 C. J. Murphy, M. R. Arkin, Y. Jenkins, N. D. Ghatlia, S. H. Bossmann, N. J. Turro, and J. K. Barton, Science **262**, 1025 (1993).
3 C. R. Treadway, M. G. Hill, and J. K. Barton, Chem. Phys. **281**, 409 (2002).
4 E. Meggers, M. E. Michel-Beyerle, , and B. Giese, J. Am. Chem. Soc. **120**, 12950 (1998).
5 E. Meggers, D. Kusch, M. Spichty, U. Wille, and B. Giese, Angew. Chem. Int. Ed. Engl. **37**, 460 (1998).
6 F. D. Lewis, X. Liu, Y. Wu, S. E. Miller, M. R. Wasielewski, R. L. Letsinger, R. Sanishvili, A. Joachimiak, V. Tereshko, and M. Egli, J. Am. Chem. Soc. **121**, 9905 (1999).
7 A. M. Brun and A. Harriman, J. Am. Chem. Soc. **116**, 10383 (1994).
8 S. O. Kelley and J. K. Barton, Science **283**, 375 (1999).
9 F. C. Grozema, Y. A. Berlin, and D. A. Siebbeles, J. Am. Chem. Soc. **122**, 10903 (2000).
10 G. B. Schuster, ed., vol. 237 of *Topics in Current Chemistry* (Springer, Berlin, 2004), ISBN 3-540-20131-9.
11 J. Jortner, M. Bixon, T. Langenbacher, and M. E. Michel-Beyerle, Proc. Natl. Acad. Sci. USA **95**, 12759 (1998).
12 K.-H. Yoo, D. H. Ha, J.-O. Lee, J. W. Park, J. Kim, J. J. Kim, H.-Y. Lee, T. Kawai, and H. Y. Choi, Phys. Rev. Lett. **87**, 198102 (2001).
13 D. Porath, A. Bezryadin, S. D. Vries, and C. Dekker, Nature **403**, 635 (2000).
14 E. Braun, Y. Eichen, U. Sivan, and G. Ben-Yoseph, Nature **391**, 775 (1998).
15 A. Y. Kasumov, M. Kociak, S. Gueron, B. Reulet, and V. T. Volkov, Science **291**, 280 (2001).
16 A. J. Storm, J. V. Noort, S. D. Vries, and C. Dekker, Appl. Phys. Lett. **79**, 3881 (2001).
17 P. Tran, B. Alavi, and G. Gruner, Phys. Rev. Lett. **85**, 1564 (2000).
18 D. Porath, G. Cuniberti, and R. D. Felice, *Charge transport in DNA-based devices*, p. 183, vol. 237 of[10] (2004).
19 R. G. Endres, D. L. Cox, and R. R. P. Singh, Rev. Mod. Phys. **76**, 195 (2004).
20 B. Xu, P. Zhang, X. Li, and N. Tao, Nano-letters **4**, 1105 (2004).
21 K. Keren, R. S. Berman, E. Buchstab, U. Sivan, and E. Braun, Science **302**, 1380 (2003).
22 M. Hazani, F. Hennrich, M. Kappes, R. Naaman, D. Peled, V. Sidorov, and D. Shvarts, Chem. Phys. Lett. **391**, 389 (2004).
23 M. Mertig, R. Kirsch, W. Pompe, and H. Engelhardt, Eur. Phys. J. D **9**, 45 (1999).
24 A. Calzolari, R. D. Felice, E. Molinari, and A. Garbesi, Appl. Phys. Lett. **80**, 3331 (2002).
25 R. Di Felice, A. Calzolari, and E. Molinari, and A. Garbesi, Phys. Rev. B **65**, 045104 (2002).
26 R. N. Barnett, C. L. Cleveland, A. Joy, U. Landman, and G. B. Schuster, Science **294**, 567 (2001).
27 F. L. Gervasio, P. Carloni, and M. Parrinello, Phys. Rev. Lett. **89**, 108102 (2002).
28 E. Artacho, M. Machado, D. Sanchez-Portal, P. Ordejon, and J. M. Soler, Mol. Phys. **101**, 1587 (2003).
29 P. J. de Pablo, F. Moreno-Herrero, J. Colchero, J. Gomez Herrero, P. Herrero, A. M. Baro, P. Ordejon, J. M. Soler, and E. Artacho, Phys. Rev. Lett. **85**, 4992 (2000).
30 S. S. Alexandre, E. Artacho, J. M. Soler, and H. Chacham, Phys. Rev. Lett. **91**, 108105 (2003).
31 J. P. Lewis, P. Ordejon, and O. F. Sankey, Phys. Rev. B **55**, 6880 (1997).
32 O. R. Davies and J. E. Inglesfield, Phys. Rev. B **69**, 195110 (2004).
33 E. B. Starikov, Phil. Mag. Lett. **83**, 699 (2003).
34 H. Wang, J. P. Lewis, and O. F. Sankey, Phys. Rev. Lett. **93**, 016401 (2004).
35 G. Fagas, A. Kambili, and M. Elstner, Chem. Phys. Lett. **389**, 268 (2004).
36 F. Palmero, J. F. R. Archilla, D. Hennig, and F. R. Romero, New J. Phys. **6**, 13 (2004).
37 S. Komineas, G. Kalosakas, and A. R. Bishop, Physical Review E **65**, 061905 (2002).
38 Z. Hermon, S. Caspi, and E. Ben-Jacob, Europhys. Lett. **43**, 482 (1998).
39 J. Yi, Phys. Rev. B **68**, 193103 (2003).
40 X. Q. Li and Y. Yan, Appl. Phys. Lett. **81**, 925 (2001).
41 G. Cuniberti, L. Craco, D. Porath, and C. Dekker, Phys. Rev. B **65**, 241314(R) (2002).
42 P. Ao, S. Grundberg, and J. Rammer, Phys. Rev. B **53**, 10042 (1996).
43 W. Zhang and S. E. Ulloa, Microelec. Journal **35**, 23 (2004).
44 P. Hänggi, S. Kohler, J. Lehmann, and M. Strass, *AC-driven transport through molecular wires* (Springer, Berlin, 2005), Lecture Notes in Physics, to appear.
45 R. Gutierrez, S. Mandal, and G. Cuniberti, `cond-mat/cond-mat/0410660`, (2004).
46 S. Tornow, N. H. Tong, and R. Bulla, `cond-mat/0405547`, (2005).
47 Y. A. Berlin, A. L. Burin, and M. A. Ratner, Superlattices and Microstructures **28**, 241 (2000).
48 F. C. Grozema, L. D. A. Siebbeles, Y. A. Berlin, and M. A. Ratner, ChemPhysChem **6**, 536 (2002).

[49] S. Roche, Phys. Rev. Lett. **91**, 108101 (2003).
[50] H. Yamada, `cond-mat/0406040` (2004).
[51] W. Zhang and S. E. Ulloa, Phys. Rev. B **69**, 153203 (2004).
[52] M. Unge and S. Stafstrom, Nano-letters **3**, 1417 (2003).
[53] Y. Zhu, C. C. Kaun, and H. Guo, Phys. Rev. B **69**, 245112 (2004).
[54] Y.-S. Jo, Y. Lee, and Y. Roh, Materials Science and Engineering **C23**, 841 (2003).
[55] T. Heim, D. Deresmes, and D. Vuillaume, `cond-mat/0405547` (2004).
[56] We speak of backbones in a very generic way. In our model the side chain (=backbones) is representative of the sugar/phosphate mantle as well as of the complementary strand. Hence, electronic states on the backbones (in our use of the term) are not necessarily localized on the sugar/phosphate molecular groups.
[57] G. Caliscan, D. Mechtani, J. H. Roh, A. Kisliuk, A. P. Sokolov, S. Azzam, M. T. Cicerone, S. Lin-Gibson, and I. Peral, J. Chem. Phys. **121**, 1978 (2004).
[58] U. Weiss, *Quantum Dissipative Systems*, vol. 10 of *Series in Modern Condensed Matter Physics* (World Scientific, 1999).
[59] G. D. Mahan, *Many-Particle Physics* (Plenum Press, New York, 2000), 3rd ed., ISBN 0-306-46338-5.
[60] S. Datta, Cambridge University Press, Cambridge (1995).
[61] Y. Imry, O. Entin-Wohlman, and A. Aharony, `cond-mat/0409075` (2004).
[62] I. S. Gradshteyn and I. M. Ryzhik, Academic Press (2000).
[63] T. Holstein, Ann. Phys. N.Y. **8**, 325 (1959).
[64] J. Gilmore, and R. McKenzie, J. Phys.:Condens. Matter **17**, 1735 (2005).
[65] D. Segal, A. Nitzan, W. B. Davies, M. R. Wasielewski, and M. A. Ratner, J. Phys. Chem. B **104**, 3817 (2000).
[66] Y. A. Berlin, A. L. Burin, and M. A. Ratner, J. Am. Chem. Soc. **123**, 260 (2001).